# ERROR ANALYSIS OF COMPOSITE SHOCK INTERACTION PROBLEMS

**T. Lee, Y. Yu, M. Zhao, J. Glimm, X. Li and K. Ye**

Department of Applied Mathematics and Statistics
State University of New York at Stony Brook
Stony Brook, NY 11794-3600
twlee,yan2000,mingzhao,glimm,linli,kye@ams.sunysb.edu

**Abstract**

We propose statistical models of uncertainty and error in numerical solutions. To represent errors efficiently in shock physics simulations we propose a composition law. The law allows us to estimate errors in the solutions of composite problems in terms of the errors from simpler ones as discussed in a previous paper. In this paper, we conduct a detailed analysis of the errors. One of our goals is to understand the relative magnitude of the input uncertainty *vs.* the errors created within the numerical solution. In more detail, we wish to understand the contribution of each wave interaction to the errors observed at the end of the simulation.

# 1 Introduction

We are concerned with the identification and characterization of solution errors in spherically symmetric shock interaction problems. This issue applies to the study of supernova and the design of inertial confinement fusion (ICF) capsules. In the first case, theory and simulations contain a number of uncertainties, and comparison to observations is thus not definitive. A systematic effort to remove or quantify some of the uncertainties associated with simulation will thus be a useful contribution. In the second case of ICF design, concern over solution accuracy has led to mandates of formal efforts to assure solution accuracy.

In previous papers, we have developed a general approach to uncertainty and numerical solution error [4, 5]. We have analyzed shock interactions in planar [1, 2] and in spherical [3] geometries. Here we focus specifically on determining the contributions of each wave interaction to the total error at any given stage in the simulation.

We studied repeated interactions of a spherically symmetric shock wave with a spherical density discontinuity layer. We performed numerical simulations on an ensemble of 200 initial conditions perturbed from a base case. The numerical solutions are obtained with mesh sizes 100, 500, and 2000. We use the difference between the fine grid solutions (2000

[1]Supported in part by the NSF Grant DMS-0102480 and the U. S. Department of Energy Grant DE-AC02-98CH10886

[2]Supported in part by the Army Research Office Grant DAAD-190110642, the U.S. Department of Energy Grant DE-FG02-90ER25084 and the U.S. Department of Energy Grant DE-FG03-98DP00206.

[3]Supported by the U.S. Department of Energy

[4]Supported in part by U.S. Department of Energy Grant DEFC02-01ER25461

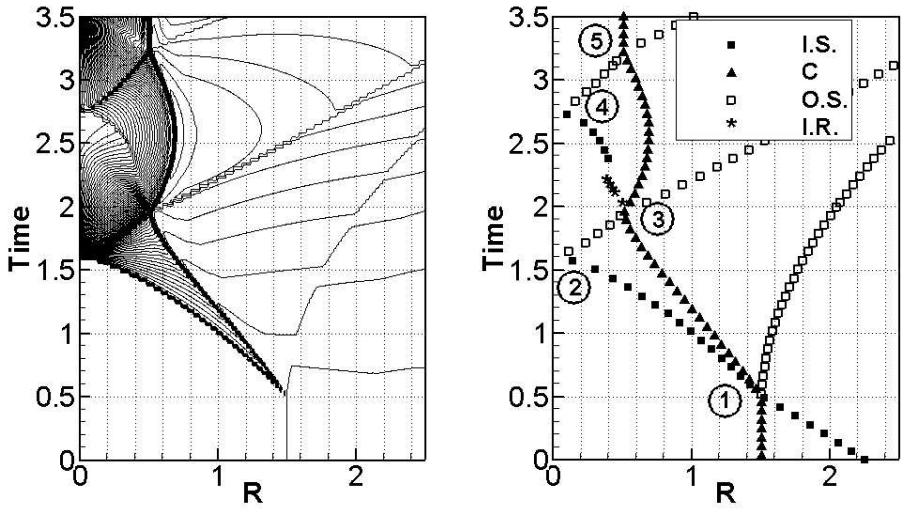


Figure 1: Left: space time density contour plot for the multiple wave interaction problem studied in this paper, in spherical geometry. Right: type and location of waves determined by the wave filter analysis with labels for the interactions. Here I.S., C, O.S., I.R. denote the inward moving shock, the contact, outward moving shock and inward moving rarefaction respectively.

mesh) and the two coarse grid solutions to represent the numerical simulation errors at the two coarse grid levels. The created solution errors in wave strength, wave width and wave positions are modeled statistically with simple linear regression models in which the input conditions are the predictors. Errors associated with the linear regression model, studied previously [1, 2], are small. Then we use a composition law, also developed previously [2, 3], to combine the statistical models for uncertainty and error at each wave interaction. We predict both the mean (bias) and standard deviation $\sigma$ of the errors. Following conventional ideas in statistics, we regard $\pm 2\sigma$ as the length of a statistical error bar for the simulation, and the mean error as giving an offset of the error bar from the coarse grid simulation. In this way we have a systematic method for the introduction of error bars for numerical errors (including input uncertainty) into numerical simulations. Here we focus on the output of the third wave interaction, i.e. after the reshock. See Fig. 1. Our predictions are compared with errors obtained directly through numerical simulation of the entire sequence of repeated shock wave interactions. Our prediction method, although simple, gives one to two significant digits in the mean solution error in all the cases except for the case of wave position errors in the 100 mesh simulation. The errors come from two sources, numerical simulation and input uncertainty, propagated and transmitted through wave interactions. We call these the created and transmitted errors for short. Note that the created errors may be created at any earlier interaction, and are then transmitted to some later interaction, where they contribute to the total error at that space time location.

## 2 The Multipath Error Analysis Formula

We develop a general formula for the error at the output to interaction $j$, in terms of the input to this interaction. By composing this formula over all previous interactions, we obtain the error at the output to interaction $j$ in terms of the initial uncertainty and the created errors at each interaction $i \leq j$. The formula thus has individual terms associated with each of the contributing wave interaction diagrams [2]. We call it the Multipath Error Analysis Formula.

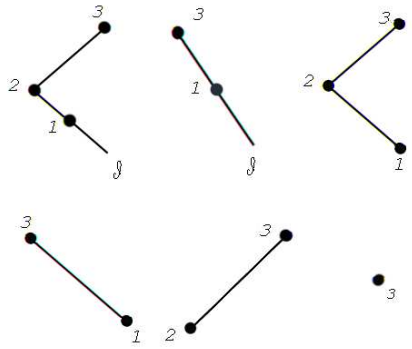


Figure 2: Schematic graphs, showing all six wave diagram contributions to the errors or uncertainty in the output from a single Riemann solution, namely the reshock interaction (numbered 3 in the right frame of Fig. 1) of the reflected shock from the origin as it crosses the contact. The numbers labeling the black circles refer to the Riemann interactions contributing to the error. The letter $\mathcal{I}$ in the first two diagrams indicates input uncertainty.

We first appeal to the fine grid simulation data (as a stand in for the exact solution) to develop or parameterize an affine linear model for the output wave strengths at interaction $j$ in terms of the input wave strengths. This formula, considered variationally, also yields a model for the transmission of error/uncertainty through interaction $j$. We additionally initialize comparable input on the fine and coarse grids at interaction $j$, so that the difference between the fine and coarse grid solutions is the created error at interaction $j$. The created error, $\mathcal{C}_s^{(j)}$, in the wave strength $w$ at interaction $j$ is thus defined as

$$\mathcal{C}_s^{(j)} = \text{coarse} - \text{fine} = w_{s(c)}^{o(j)} - w_{s(f)}^{o(j)} \quad .$$

Here the three output waves are indexed form left to right by $s$, $1 \leq s \leq 3$. The superscripts $o$ and $i$ represent output and input strengths respectively, and the subscripts $f$ and $c$ represent fine and coarse grid solutions.

The linear regression, or linear approximate formula for the output wave strength at interaction $j$ is obtained from the fine grid simulation data,

$$w_{s(f)}^{o(j)} = \alpha_s^{(j)} + \sum_{k=1}^{2} \beta_{sk}^{(j)} w_{k(f)}^{i(j)} \quad . \tag{1}$$

We use this formula variationally to obtain a formula for the transmission of input error $\delta w_k^{i(j)}$. The input error itself is a combination of transmitted input uncertainties $\mathcal{I}_c, \mathcal{I}_s$ and created errors $\mathcal{C}_s^{(i)}$ also transmitted from interactions $i < j$,

$$\delta w_{s(f)}^{o(j)} = \sum_{k=1}^{2} \beta_{sk}^{(j)} \delta w_k^{i(j)} \quad . \tag{2}$$

A source $\mathcal{S}_r^{(i)}$ of errors contributes to the output error through wave interaction diagrams $g \in \mathcal{G}_{(i)r}^{(j)s}$, which connect the $r$th source at interaction $i$ to the $s$th output at the interaction $j$. Such diagrams were introduced in [2]. A shock wave as input to an intermediate interaction $m$ with radius $r^{(m)}$ in a diagram $g \in \mathcal{G}$ is propagated from the previous interaction $m\prime$ occurring at the radius $r^{(m\prime)}$ according to a power law. The power law gives the definition of a propagator with a proper power $a^{(m,g)}$ for the $m\prime$ $m$ bond of the diagram $g$,

$$\mathcal{P}_{(m\prime)}^{(m)} = \left( \frac{r^{(m)}}{r^{(m\prime)}} \right)^{a^{(m,g)}} \quad . \tag{3}$$

We define $\gamma_{sk}^{(m)}$ for the $s$th output and the $k$th input at interaction $m$ as the multiple of a coefficient and a propagator, which are defined by a bond in the diagram $g$ (*i.e.*$\beta$ is related to $g$ and $\mathcal{P}$ to $g$)

$$\gamma_{sk}^{(m)} = \beta_{sk}^{(m)} \mathcal{P}_{(m\prime)}^{(m)} \quad .$$

The coarse grid output error is the sum of the transmitted errors from (2) and the error created at interaction $j$,

$$\delta w_{s(c)}^{o(j)} = \sum_{\substack{1 \le r \le 3 \\ 0 \le i \le j}} \sum_{g \in \mathcal{G}_{(i)r}^{(j)s}} \mathcal{C}_g \mathcal{S}_r^{(i)} \quad , \tag{4}$$

where $\mathcal{C}_g = \prod_{\mathcal{B}(g)} \gamma_{sk}^{(m)}$ and the product runs over all bonds $\mathcal{B}(g)$ of the diagram $g$. Observe that the created error at interaction $j$ is included in the $i = j$ term in (4).

At the output to the interaction 3, we have the following closed form expression for the mean,

$$\langle \delta w_{s(c)}^{o(3)} \rangle = \gamma_{s1}^{(3)} \gamma_{11}^{(2)} \langle \mathcal{C}_1^{(1)} \rangle + \gamma_{s2}^{(3)} \langle \mathcal{C}_2^{(1)} \rangle + \gamma_{s1}^{(3)} \langle \mathcal{C}_1^{(2)} \rangle + \langle \mathcal{C}_s^{(3)} \rangle \quad . \tag{5}$$

Observe that $\langle \mathcal{I}_s \rangle = \langle \mathcal{I}_c \rangle = 0$, so that with a linear propagation model and assumed mean zero initial uncertainty, the two initial uncertainties do not contribute to the mean error. We assume statistical independence of the sources, to obtain a closed form expression for the variance of the error,

$$\begin{aligned} \text{Var } \delta w_{s(c)}^{o(3)} \quad = \quad & \left\{ \left( \gamma_{s1}^{(3)} \gamma_{11}^{(2)} \gamma_{11}^{(1)} \right)^2 + \left( \gamma_{s2}^{(3)} \gamma_{21}^{(1)} \right)^2 \right\} \text{Var } \mathcal{I}_c \\ & + \left\{ \left( \gamma_{s1}^{(3)} \gamma_{11}^{(2)} \gamma_{12}^{(1)} \right)^2 + \left( \gamma_{s2}^{(3)} \gamma_{22}^{(1)} \right)^2 \right\} \text{Var } \mathcal{I}_s \\ & + \left( \gamma_{s1}^{(3)} \gamma_{11}^{(2)} \right)^2 \text{Var } \mathcal{C}_1^{(1)} + \left( \gamma_{s2}^{(3)} \right)^2 \text{Var } \mathcal{C}_2^{(1)} + \left( \gamma_{s1}^{(3)} \right)^2 \text{Var } \mathcal{C}_1^{(2)} + \text{Var } \mathcal{C}_s^{(3)} \quad . \end{aligned} \tag{6}$$

# 3 Results

In Figs. 3, 4, we present three pie charts representing fractional contribution from each of the six interactions to the error variance for the inward rarefaction, contact and outward shock, respectively, as output to interaction 3. From these charts, we can infer the relative importance between the input uncertainty and the solution error and determine the contribution of each interaction to the total error variance.

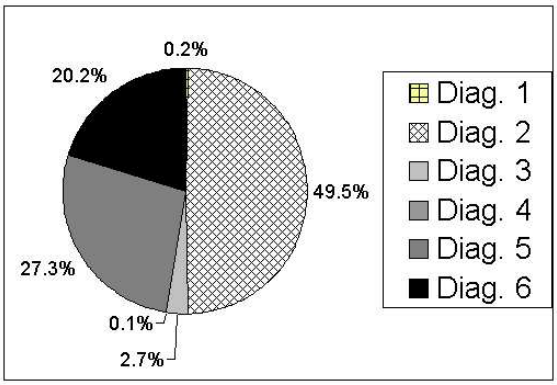


(a) Inward Rarefaction

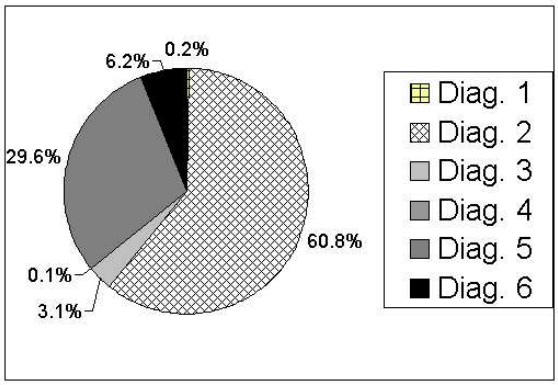


(b) Contact

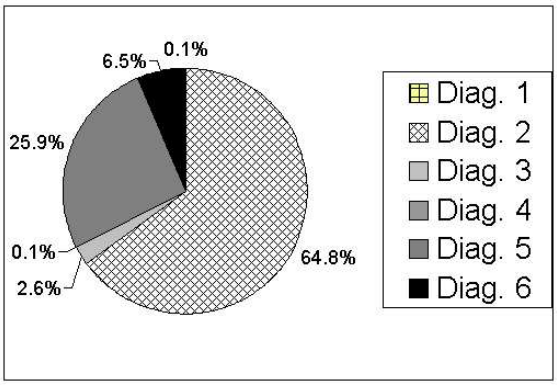


(c) Outward Shock

Figure 3: Pie charts showing the contribution of each wave interaction diagram to the error variance of the wave strength at the output of interaction 3, for a solution using 500 mesh units.

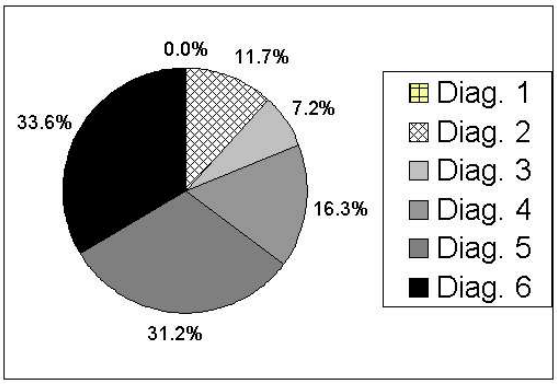


(a) Inward Rarefaction

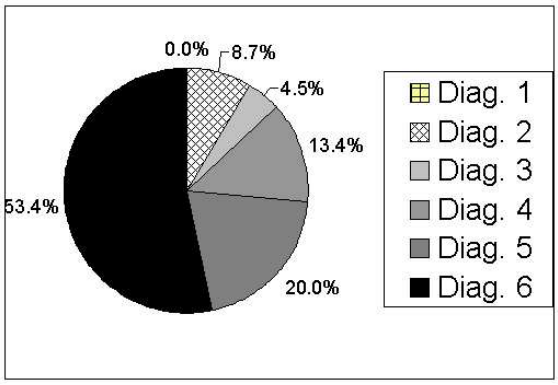


(b) Contact

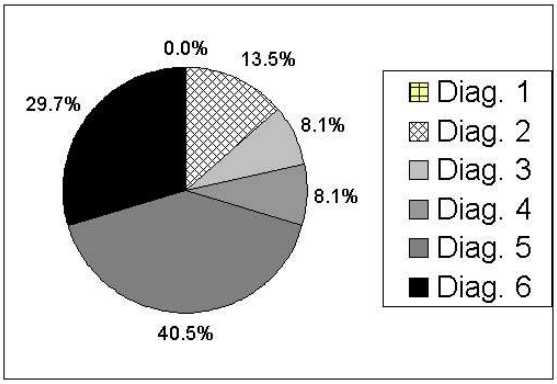


(c) Outward Shock

Figure 4: Pie charts showing the contribution of each wave interaction diagram to the error variance of the wave strength at the output of interaction 3, for a solution using 100 mesh units.

We also show the contributions of each interaction to the mean value of the final total error. See Table. 1. We only show the values corresponding to diagram 3 to 6, as the contribution of the first two diagrams (input uncertainties) is observed to be zero.

| Wave Diagram | I.R. | | C. | | O.S. | |
|---|---|---|---|---|---|---|
| Number | 100 | 500 | 100 | 500 | 100 | 500 |
| 3 | 0.10 | -0.01 | -0.01 | 0.001 | 0.09 | -0.009 |
| 4 | 0.05 | 0.009 | 0.1 | 0.02 | -0.02 | -0.004 |
| 5 | -0.05 | -0.005 | 0.006 | 0.0006 | -0.04 | -0.004 |
| 6 | -0.07 | 0.015 | 0.03 | 0.01 | -0.05 | 0.01 |
| Total Prediction | 0.03 | 0.009 | 0.12 | 0.03 | -0.02 | -0.007 |
| Total Simulation | 0.04 | 0.01 | 0.14 | 0.03 | -0.02 | -0.006 |

Table 1: The contribution of each interaction to the mean value of the total error in each of three output waves at the output to interaction 3, for 100 and 500 mesh units. Units are dimensionless and represent the error expressed as a fraction of the total wave strength. The last two rows compare the total of the mean error as given by the model to the directly observed mean error. The columns I.R., C., and O. S. are labeled as in Fig. 1, Right frame.

# References


[1] B. DeVolder, J. Glimm, J. W. Grove, Y. Kang, Y. Lee, K. Pao, D. H. Sharp, and K. Ye, *Uncertainty quantification for multiscale simulations*, Journal of Fluids Engineering, 124 (2002), pp. 29–41. LANL report No. LA-UR-01-4022.

[2] J. Glimm, J. W. Grove, Y. Kang, T. Lee, X. Li, D. H. Sharp, Y. Yu, K. Ye, and M. Zhao, *Statistical riemann problems and a composition law for errors in numerical solutions of shock physics problems*, SISC (In Press), (2003). University at Stony Brook Preprint Number SB-AMS-03-11, Los Alamos National Laboratory number LA-UR-03-2921.

[3] ——, *Errors in numerical solutions of spherically symmetric shock physics problems*, Contemporary Mathematics, (2004). (submitted) University at Stony Brook Preprint Number SB-AMS-04-03, Los Alamos National Laboratory number LA-UR-04-0713.

[4] J. Glimm and D. H. Sharp, *Stochastic methods for the prediction of complex multiscale phenomena*, Quarterly J. Appl. Math., 56 (1998), pp. 741–765.

[5] ——, *Prediction and the quantification of uncertainty*, Physica D, 133 (1999), pp. 152–170.